Japanese Journal of Veterinary Research 70(2): 57-63, 2022

JJVR

SHORT COMMUNICATION Experimental Research

Evaluation of the central lymphatic vessel size using non-contrast-enhanced magnetic resonance lymphography in dogs with intestinal lymphangiectasia

Takuro Nagahara[1)], Koichi Ohno[1)], Itsuma Nagao[1)], Taisuke Nakagawa[2)], Nozomu Yokoyama[3)], Kie Yamamoto[2)], Reina Fujiwara[2)], Yuko Goto-Koshino[2)], James K. Chambers[4)], Kazuyuki Uchida[4)], Yasuyuki Momoi[5)], Hirotaka Tomiyasu[1,*)] and Hajime Tsujimoto[1)]

[1)] Department of Veterinary Internal Medicine, Graduate School of Agricultural and Life Sciences, The University of Tokyo, 1-1-1 Yayoi, Bunkyo-ku, Tokyo 113-8657, Japan

[2)] Veterinary Medical Center, Graduate School of Agricultural and Life Sciences, The University of Tokyo, 1-1-1 Yayoi, Bunkyo-ku, Tokyo 113-8657, Japan

[3)] Veterinary Teaching Hospital, Graduate School of Veterinary Medicine, Hokkaido University, N18 W9, Kita-ku, Sapporo, Hokkaido 060-0818, Japan

[4)] Laboratory of Veterinary Pathology, Graduate School of Agricultural and Life Sciences, The University of Tokyo, 1-1-1 Yayoi, Bunkyo-ku, Tokyo 113-8657, Japan

[5)] Department of Veterinary Clinical Pathobiology, Graduate School of Agricultural and Life Sciences, The University of Tokyo, 1-1-1 Yayoi, Bunkyo-ku, Tokyo 113-8657, Japan

Received for publication, November 16, 2021; accepted, April 2, 2022

Abstract

Intestinal lymphangiectasia (IL) is a common complication in dogs. In human medicine, abnormalities in central lymphatic vessels are associated with IL. Thus, we evaluated central lymphatic vessels using non-contrast-enhanced magnetic resonance lymphography in dogs with IL. Twelve dogs with IL confirmed by gastrointestinal endoscopy were included. Five dogs were diagnosed with lymphoplasmacytic enteritis, three with small-cell lymphoma, and four with large-cell lymphoma. There was no significant difference in the size of the thoracic duct, cisterna chyli, and lumbar lymphatic trunk between control and dogs with IL ($P > 0.05$). Thus, the central lymphatic vessel dilation is not observed even in dogs with IL, suggesting that IL is confined to the small intestinal tissues.

Key Words: central lymphatic vessel, intestinal lymphangiectasia, non-contrast-enhanced magnetic resonance lymphography

The intestinal lymphangiectasia (IL) is a common complication in dogs with chronic small intestinal diseases, including lymphoplasmacytic enteritis and small-cell and large-cell gastrointestinal lymphomas[11)]. In dogs with IL, the lymph leakage into the small intestinal lumen leads to protein-losing enteropathy (PLE). Previous histopathological studies have shown that lymphatic vessels dilate in the transmural layers of the intestine[7,15)]. The lymph absorbed

* Corresponding author: Hirotaka Tomiyasu
Address: Department of Veterinary Internal Medicine, Graduate School of Agricultural and Life Sciences, The University of Tokyo, 1-1-1 Yayoi, Bunkyo-ku, Tokyo 113-8657, Japan
Fax number: +81-3-5841-5403. E-mail address: atomi@g.ecc.u-tokyo.ac.jp
doi: 10.14943/jjvr.70.2.57

by small intestinal lacteals flows into mesenteric collecting vessels that unite with the lumbar lymphatic trunk and hepatic lymphatic vessel in the retroperitoneum, forming cisterna chyli. It then passes through the thoracic duct to transport lymph to the venous system[5].

Lymph fluid is transported by spontaneous contraction of the lymph vessels themselves and the contraction of skeletal and smooth muscles outside of lymph vessels. Spontaneous contractions of lymphatic vessels are observed in mice, rats, guinea pigs, and humans but are very weak in dogs[1,14]. Therefore, the capacity of canine lymphatic vessels to transport lymph fluid might be lower than those in other species, and it is possible that such lower contraction ability of the lymphatic vessels in dogs might be one of the causes of lymphatic congestions leading to the occurrence of IL, since IL is highly prevalent in dogs but is rare in other animal species such as humans. Based on these backgrounds, we speculated that systemic abnormalities in lymphatic vessels lead to lymphatic congestion contributing to canine IL, and the central lymphatic vessels are dilated as those in intestines in dogs with IL.

The thoracic duct and cisterna chyli can be identified by non-contrast-enhanced magnetic resonance (MR) lymphography, although its usefulness has not been compared with other techniques such as CT lymphography in veterinary medicine[8]. Non-contrast-enhanced MR lymphography has several benefits, despite the disadvantage of a low spatial resolution compared with computed tomography (CT) lymphography. First, the injection of contrast medium and massage of administration sites are unnecessary, avoiding adverse events. Moreover, lymphatic flow and the scan timing would not be affected by the contrast agent injection. Therefore, we used non-contrast-enhanced MR lymphography to evaluate the central lymphatic vessel, including the thoracic duct, cisterna chyli, lumbar lymphatic trunk, and mesenteric lymphatic vessel in dogs with IL.

Dogs who performed both gastrointestinal endoscopy and CT examination from March to November 2019 at the Veterinary Medical Center of the University of Tokyo were included. Of them, dogs histopathologically diagnosed with IL were finally included in this study. Mucosal biopsy samples obtained by gastrointestinal endoscopy were fixed in 10% neutral buffered formalin and embedded by paraffin. Hematoxylin eosin-stained sections were used for diagnosis. Lymphoplasmacytic enteritis was diagnosed according to the histopathological standards of the World Small Animal Veterinary Association (WSAVA)[4]. Small-cell and large-cell lymphomas were diagnosed according to the World Health Organization's lymphoma diagnostic criteria in conjunction with the descriptions in recent studies on canine small-cell lymphoma[3,11]. In addition, the severity of IL was assessed by the ratio of the villus lacteal width to that of the lamina propria according to the WSAVA guidelines[4]. Medical records were reviewed for each dog, and the following information was collected: breed, sex, age, body weight, clinical signs, vertebral heart size (VHS), clinicopathological data, and CT findings.

Eight dogs were used as a control group. Four healthy beagles owned by the University of Tokyo were included as control dogs. The experimental and animal care procedures were approved by the Animal Use and Care Committee of the University of Tokyo (P19-014). We also included three dogs that underwent MRI because of neck pain, back pain, and seizure and one that underwent CT because of the intestinal foreign body. Their breeds were Beagle, Labrador Retriever, Miniature Dachshund, and Toy Poodle, respectively. There were two spayed females and two castrated males with a median body weight of 9.52 kg (range; 5.8–23.0 kg). Informed consent was obtained from all owners to perform MRI as a clinical examination.

Twelve dogs with IL were finally included in the present study. Based on the histopathological examination, five dogs were diagnosed with

lymphoplasmacytic enteritis, three with small-cell lymphoma, and four with large-cell lymphoma. Nine dogs had mild IL, and 3 had moderate IL. The breeds consisted of three Shibas, two Miniature Dachshunds, two Welsh Corgi Pembrokes, and one of French Bulldog, Jack Russell Terrier, Pug, Shih Tzu, and Yorkshire Terrier. There were five castrated males, six spayed females, and one intact female. The median age was 9.9 years old (range; 1.8–14.4 years old). The clinical signs associated with the gastrointestinal disease were as follows: diarrhea (n=9), weight loss (n=8), lethargy (n=7), anorexia (n=7), and vomiting (n=4), respectively. One dog had a VHS value of 11, suggesting cardiac dilation, but the case showed no abnormality in echocardiography. In the CT examination, ascites (n=5), swelling of mesenteric lymph nodes (n=4), congenital portosystemic shunt (n=1), swelling of parasternal lymph node (n=1), pulmonary thrombosis (n=1), and arterial thrombosis (n=1) were detected. No mass lesion in the pleural cavity, affecting central lymphatic vessel size, was observed in any dogs. The median body weight of the dogs with IL was 4.5 kg (range; 3.2–9.6 kg), which was significantly lower than 11.0 kg (range; 5.8–23.0 kg, $P < 0.001$ in Mann–Whitney U test) in the control dogs. The median plasma albumin concentration in dogs with IL was 2.0 g/dl (range; 1.1–2.5 g/dl), and significantly lower than the median value of 3.7 g/dl (range; 3.4–4.1 g/dl, $P < 0.001$ in Mann–Whitney U test) in the control dogs.

The non-contrast-enhanced MR lymphography was performed before gastrointestinal endoscopy and CT examination to perform these examinations in the same anesthesia and to avoid the effects of contrast medium injection. Non-contrast-enhanced MR lymphography was performed using a 3.0 T MR unit (Vantage Galan 3T, Canon Medical Systems, Tochigi, Japan). 3D single-shot fast spin-echo as non-contrast-enhanced MR lymphography (TR = 4,001 msec, TE = 601 msec, echo train length = 1, field of view (FOV) = 250 × 180 mm, thickness = 1 mm, spatial resolution = 0.62 × 0.62 mm, slice number = 60) was performed with respiratory gating, and images were obtained during exhalation. The imaging time in this study was 15–20 min.

One of the four healthy beagle dogs was used to validate the visualization of central lymphatic vessels by non-contrast-enhanced MR lymphography. Non-contrast-enhanced MR lymphography was performed as described above. CT lymphography was performed as previously reported with minor modifications[10]. First, 1.0 ml/kg of contrast medium (Iohexol, 300 mg Iodine/mL, Iopaque 300, Fuji Pharma, Tokyo, Japan) was injected into the intrametatarsal pad, and the administration site was massaged for 10 min. Then, CT imaging was carried out using an 80-row multi-slice CT scanner (Aquilion Prime; Canon Medical Systems). The scanning settings were 120 kV, 50–300 mA, 0.5 sec tube rotation time, 65.0 helical pitch, 240.0–500.0 mm FOV, and 512 × 512 matrices. Images of CT and non-contrast-enhanced MR lymphography were overlaid based on the vertebrae and cerebrospinal fluid (CSF) using workstations (Vitrea, Canon Medical Systems).

The images of non-contrast-enhanced MR lymphography in one healthy beagle dog are shown in Fig. 1. The lymphatic vessel, isointense to the CSF, was found around the aorta in the transverse image (Fig. 1A and C). The thoracic duct, cisterna chyli, and lumbar lymphatic trunk were identified in the sagittal images (Fig. 1B and D). The transverse and sagittal images of lymphatic vessels obtained by non-contrast-enhanced MR lymphography overlapped well with those obtained by CT lymphography (Fig. 1E and F). We also tried to describe the mesenteric lymphatic vessels as vessels consecutive to the cisterna chyli, but they could not be distinguished from the intestinal juice or ascites. Therefore, the lymphatic vessel size was evaluated for the thoracic duct, cisterna chyli, and lumbar lymphatic trunk, not for the mesenteric lymphatic vessel.

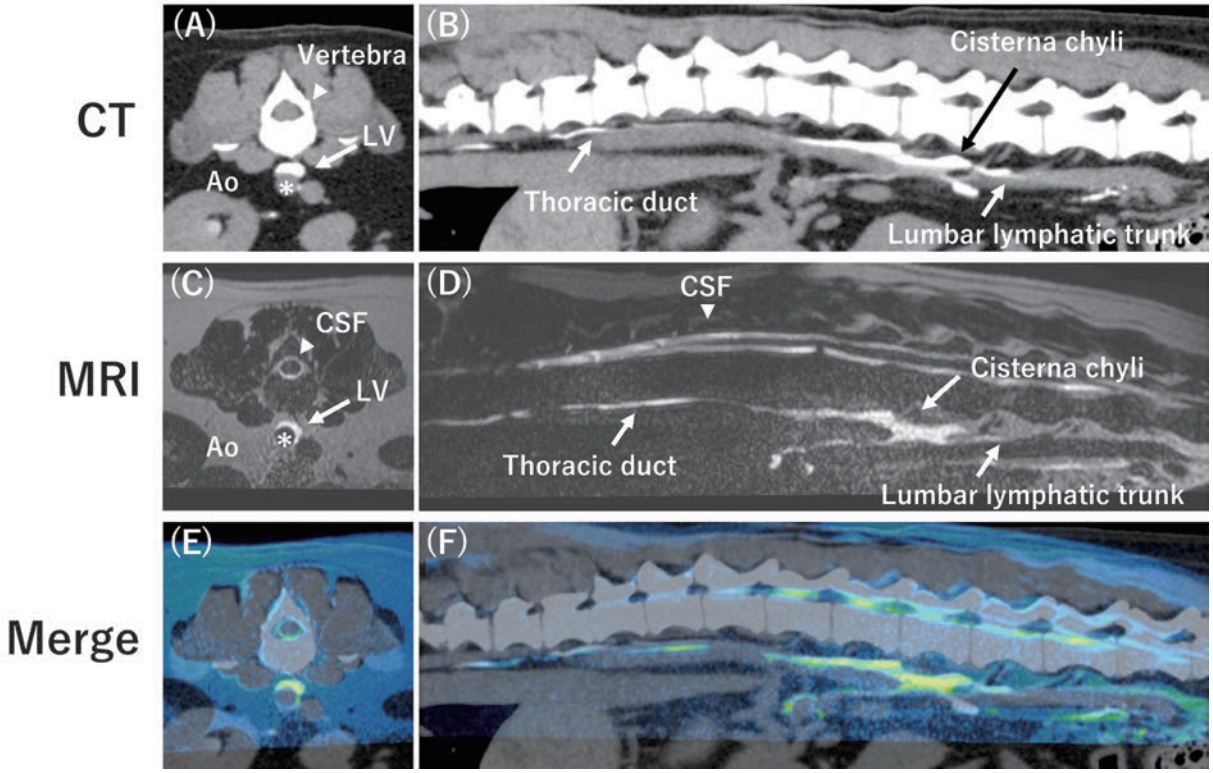

Fig. 1. Transverse and sagittal images of computed tomography (CT) (A and B) and non-contrast-enhanced magnetic resonance lymphography (MRI) (C and D) were obtained in a healthy beagle dog. These images were overlaid based on the vertebra and cerebrospinal fluid (E and F). The lymphatic vessel (arrows) was found around the aorta (asterisk) and ventral to the vertebra (arrowhead in A) or cerebrospinal fluid (arrowhead in C). The cisterna chyli was identified by the retroperitoneal dilated lymphatic channel adjacent to the aorta. The lymphatic vessel cranial to the cisterna chyli was recognized as the thoracic duct, and that caudal to the cisterna chyli was recognized as the lumbar lymphatic trunk (B and D). Ao, aorta; CSF, cerebrospinal fluid; LV, lymphatic vessel.

The lymphatic vessel size was evaluated in transverse images orthogonal to CSF. Because the lymphatic vessels have irregular forms, we used cross-sectional area instead of thickness. The cross-sectional area was measured by manually marking the lymphatic vessels on the image software (Osirix DICOM Viewer, Pixmeo SARL, Switzerland). If there was more than one lymphatic vessel in an image, the sum of the cross-sectional area of all lymphatic vessels was calculated. To correct the influence of body size, the cross-sectional area of the aorta was also measured at the same slices. First, we identified cisterna chyli, retroperitoneal dilated lymphatic channels adjacent to the aorta. In the present study, cisterna chyli was identified in the range of L2 to L4, with the most frequency in L3. The cisterna chyli cross-sectional area to aorta ratio was evaluated in the most extended part of the cisterna chyli. We then identified the thoracic duct and lumbar lymphatic trunk based on the location of the cisterna chyli. The lymphatic vessel cranial to the cisterna chyli was the thoracic duct, and that caudal to the cisterna chyli was the lumbar lymphatic trunk. The lymphatic vessel cross-sectional area to aorta ratio was measured at each mid vertebral region from T11 to L5, and lymphatic vessel sizes of the thoracic duct and lumbar lymphatic trunk were calculated by averaging the cross-sectional area to aorta ratios in regions corresponding to the thoracic duct and lumbar lymphatic trunk, respectively. The evaluation of non-contrast-enhanced MR lymphography images and calculation of the

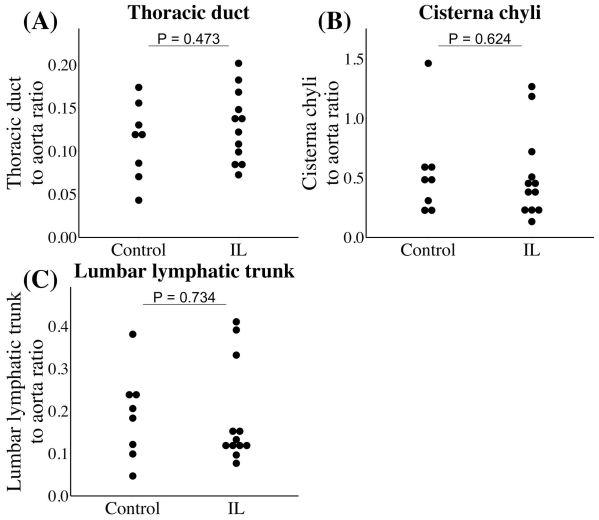

Fig. 2. Dot plots of the central lymphatic vessel to aorta ratio in cross-sectional area in the control and dogs with intestinal lymphangiectasia (IL). There was no significant difference in thoracic duct (A), cisterna chyli (B), and lumbar lymphatic trunk (C) to aorta ratio between control and dogs with IL ($P > 0.05$ in Mann–Whitney U test)

lymphatic vessel size was repeated three times in each dog. The coefficient of variations (CV) was calculated using the following formula: CV = standard deviation / mean × 100.

The lymphatic vessel cross-sectional area ranged from 1.1–73.4 mm^2. The median CVs for the evaluation of central lymphatic vessel size was as follows: thoracic duct (9.1 %, range; 2.5–17.9 %), cisterna chyli (9.2 %, range; 1.5–15.6 %), and lumbar lymphatic trunk (9.3 %, range; 0.5–24.9 %). The dot plots of the cross-sectional ratio of the lymphatic vessel to the aorta in control dogs and dogs with IL are shown in Fig. 2. The median value of the cross-sectional ratio of the lymphatic vessel to the aorta in dogs with IL was as follows: thoracic duct (0.13, range; 0.07–0.20), cisterna chyli (0.41, range; 0.13–1.27) and lumbar lymphatic trunk (0.13, range; 0.08–0.41). In contrast, the ratio in control dogs was as follows: thoracic duct (0.12, range; 0.04–0.17), cisterna chyli (0.49, range; 0.20–1.46) and lumbar lymphatic trunk (0.19, range; 0.05–0.38). Contrary to our hypothesis, there was no significant difference in central lymphatic vessel size (thoracic duct, $P = 0.473$; cisterna chyli, $P = 0.624$; lumbar lymphatic trunk, $P = 0.734$ in Mann–Whitney U test) between control dogs and dogs with IL. Moreover, the comparison between dogs with mild and moderate IL showed no significant difference in the thoracic duct, cisterna chyli, and lumbar lymphatic trunk size ($P = 1.0$ in Mann–Whitney U test).

Contrary to our hypothesis, central lymphatic vessels were not dilated in dogs with IL, and it was suggested that IL was not systemically distributed but was confined to the small intestinal tissues. Several causes could be thought to induce such confined IL. First, the lymphatic vessels may be obstructed by inflammatory or tumor cells infiltrating the small intestine associated with lymphoplasmacytic enteritis or gastrointestinal lymphoma, which are the major underlying diseases of IL. In addition, since inflammatory cytokines such as tumor necrosis factor (TNF)-α are known to decrease lymphatic contraction[2], inflammation might be directly related to lymphatic congestion and lymphatic vessel dilation, although the changes in inflammatory cytokine expressions have been controversial in dogs with chronic enteritis[6]. The causes of IL might also occur in the mesenteric lymph vessels or lymph nodes, which could not be evaluated in this study. Indeed, the obstruction of mesenteric lymphatic vessels is observed in dogs with granulomatous lymphangitis[9]. Therefore, future studies are needed to evaluate the lymphatic vessels in the small intestine and mesentery in dogs with IL.

Although this study did not suggest dilations in central lymphatic vessels, it is still possible that systemic lymphatic congestion occurred in dogs with IL because the functions of the lymphatic vessel, including lymphatic transport, could not be evaluated in this study. Time-Spatial Labeling Inversion Pulse (Time-SLIP), an imaging technique of MRI, can evaluate fluid flow and is used to evaluate CSF and lymphatic transportation in humans[12,13], and future study using this technique is needed for functional

assessment of central lymphatic transportation in dogs with IL.

This study has several limitations. First, the dogs with IL mainly comprised small breed dogs in contrast to the control dogs; therefore, the bodyweight of the control dogs was significantly higher than dogs with IL. The small sample size is also one of the limitations of the present study.

In conclusion, the central lymphatic vessel could be visualized by non-contrast-enhanced MR lymphography, which was confirmed by comparison with CT lymphography. The results in this study showed that central lymphatic vessels were not dilated even in dogs with IL, suggesting that IL is confined to the small intestine. Further studies focusing on the abnormalities in lymphatic vessels in the small intestinal tissues are needed to clarify the pathology of IL in dogs.

Acknowledgments

This work was supported by a grant-in-aid for the Japan Society for the Promotion of Science Fellows (19J22813).

References

1) Armenio S, Cetta F, Tanzini G, Guercia C. Spontaneous contractility in the human lymph vessels. Lymphology 14, 173–178, 1981.
2) Chen Y, Rehal S, Roizes S, Zhu HL, Cole WC, von der Weid PY. The pro-inflammatory cytokine TNF-α inhibits lymphatic pumping via activation of the NF-ϰB-iNOS signaling pathway. Microcirculation 24, 1–13, 2017.
3) Couto KM, Moore PF, Zwingenberger AL, Willcox JL, Skorupski KA. Clinical characteristics and outcome in dogs with small cell T-cell intestinal lymphoma. Vet Comp Oncol 16, 337–343, 2018.
4) Day MJ, Bilzer T, Mansell J, Wilcock B, Hall EJ, Jergens A, Minami T, Willard M, Washabau R. Histopathological standards for the diagnosis of gastrointestinal inflammation in endoscopic biopsy samples from the dog and cat: a report from the World Small Animal Veterinary Association Gastrointestinal Standardization Group. J Comp Pathol 138, 1–43, 2008.
5) Hokkanen K, Tirronen A, Ylä-Herttuala S. Intestinal lymphatic vessels and their role in chylomicron absorption and lipid homeostasis. Curr Opin Lipidol 30, 370–376, 2019.
6) Jergens AE, Sonea IM, O'Connor AM, Kauffman LK, Grozdanic SD, Ackermann MR, Evans RB. Intestinal cytokine mRNA expression in canine inflammatory bowel disease: a meta-analysis with critical appraisal. Comp Med 59, 153–62, 2009.
7) Kleinschmidt S, Meneses F, Nolte I, Hewicker-Trautwein M. Retrospective study on the diagnostic value of full-thickness biopsies from the stomach and intestines of dogs with chronic gastrointestinal disease symptoms. Vet Pathol 43, 1000–1003, 2006.
8) Kutara K, Kanda T, Maeta N, Mochizuki Y, Ono F, Itoh Y, Asanuma T. Combining non-contrast enhanced magnetic resonance thoracic ductography with vascular contrast-enhanced computed tomography to identify the canine thoracic duct. Open Vet J 10, 68–73, 2020.
9) Lecoindre A, Lecoindre P, Cadoré JL, Chevallier M, Guerret S, Derré G, Mcdonough SP, Simpson KW. Focal intestinal lipogranulomatous lymphangitis in 10 dogs. J Small Anim Pract 57, 465–471, 2016.
10) Lin LS, Chiu HC, Nishimura R, Fujiwara R, Chung CS. Computed tomographic lymphangiography via intra-metatarsal pad injection is feasible in dogs with chylothorax. Vet Radiol Ultrasound 61, 435–443, 2020.
11) Nakashima K, Hiyoshi S, Ohno K, Uchida K, Goto-Koshino Y, Maeda S, Mizutani N, Takeuchi A, Tsujimoto H. Prognostic factors in dogs with protein-losing enteropathy. Vet J 205, 28–32, 2015.

12) Ohtonari T, Nishihara N, Ota S, Tanaka A. Novel assessment of cerebrospinal fluid dynamics by time-spatial labeling inversion pulse magnetic resonance imaging in patients with Chiari malformation type I. World Neurosurg 112, e165–e171, 2018.
13) Rane S, Donahue PMC, Towse T, Ridner S, Chappell M, Jordi J, Gore J, Donahue MJ. Clinical feasibility of noninvasive visualization of lymphatic flow with principles of spin labeling MR imaging: implications for lymphedema assessment. Radiology 269, 893–902, 2013.
14) Smith RO. Lymphatic contractility; a possible intrinsic mechanism of lymphatic vessels for the transport of lymph. J Exp Med 90, 497–509, 1949.
15) Wennogle SA, Priestnall SL, Suárez-Bonnet A, Soontararak S, Webb CB. Lymphatic endothelial cell immunohistochemical markers for evaluation of the intestinal lymphatic vasculature in dogs with chronic inflammatory enteropathy. J Vet Intern Med 33, 1669–1676, 2019.